

A 69% Gain Improvement, 90 mV Cold-Startup, 95.2% Tracking Efficient MPPT, and I-ZCS using Maximum Output Voltage Tracking with Shared Inductor

Muhammad Ali, and Jong-Wook Lee

School of Electronics and Information, Kyung Hee University, ali.turi@khu.ac.kr

I. INTRODUCTION

This paper presents the design of a DC-DC boost converter IC system for a thermoelectric generator (TEG) using an off-chip inductor specifically intended for wearable electronics and IoT devices [1]. We propose a cold startup using a tri-state buffer to achieve high gain and linear voltage transfer characteristics (VTC) for low-voltage TEG. Furthermore, unlike previous designs [2], [3], which use zero current sensing (ZCS) based on inductor current or voltage to prevent backflow, our proposed system employs indirect-zero current sensing (I-ZCS) through maximum output voltage tracking (MOVT) to avoid inductor backflow.

II. DESCRIPTION

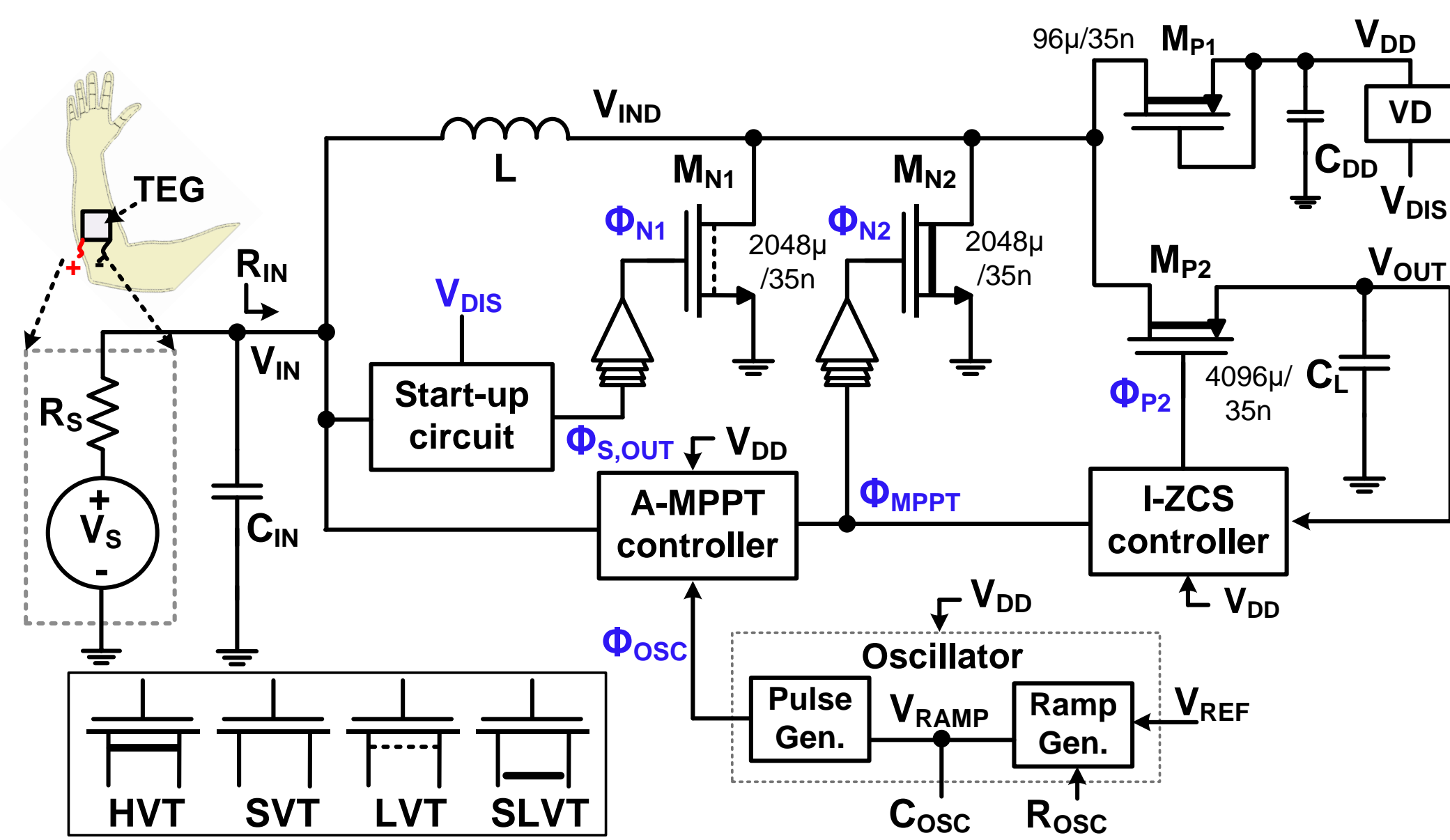


Fig. 1. Simplified schematic of the proposed system architecture.

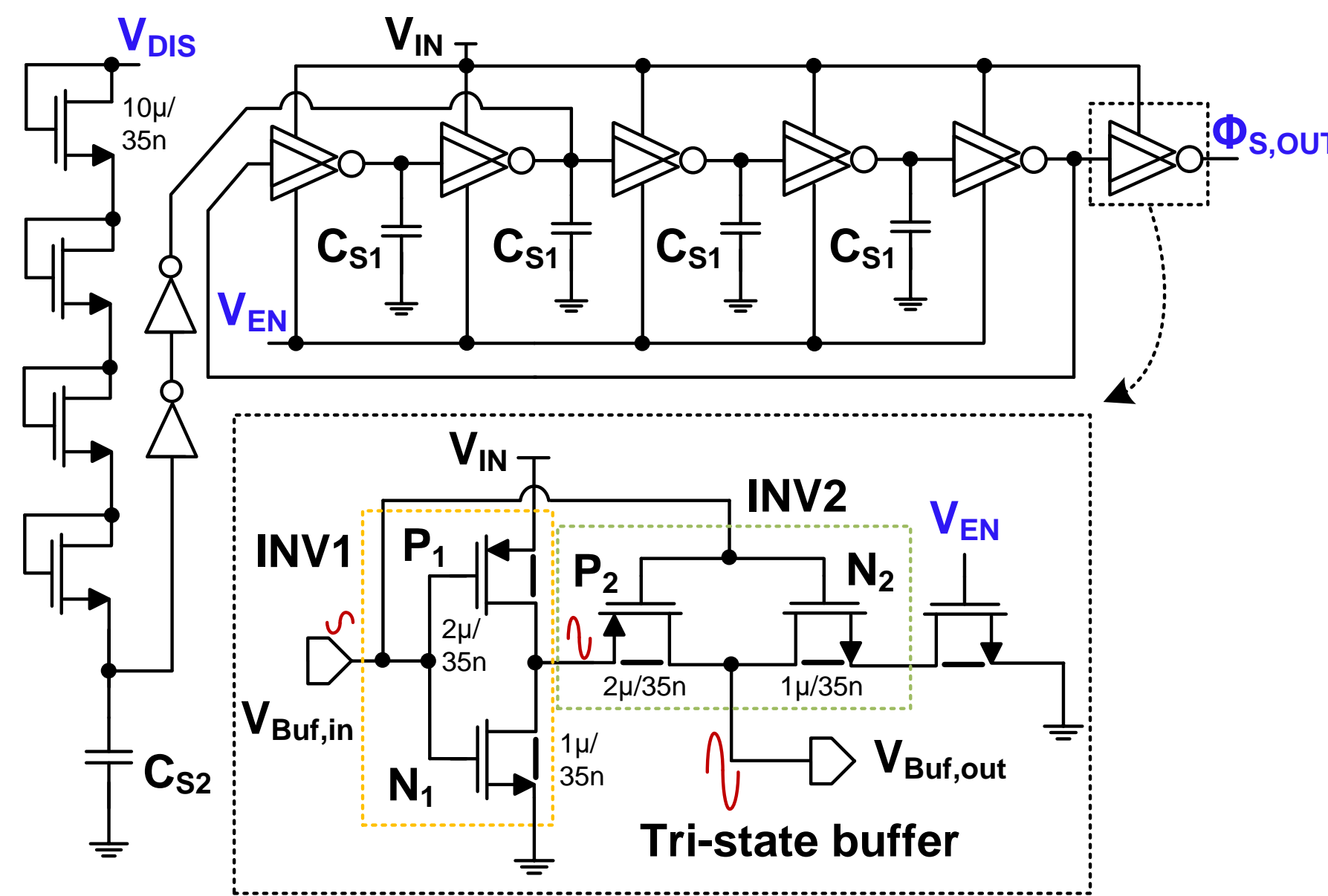


Fig. 2. Schematic of the proposed cold-startup circuit

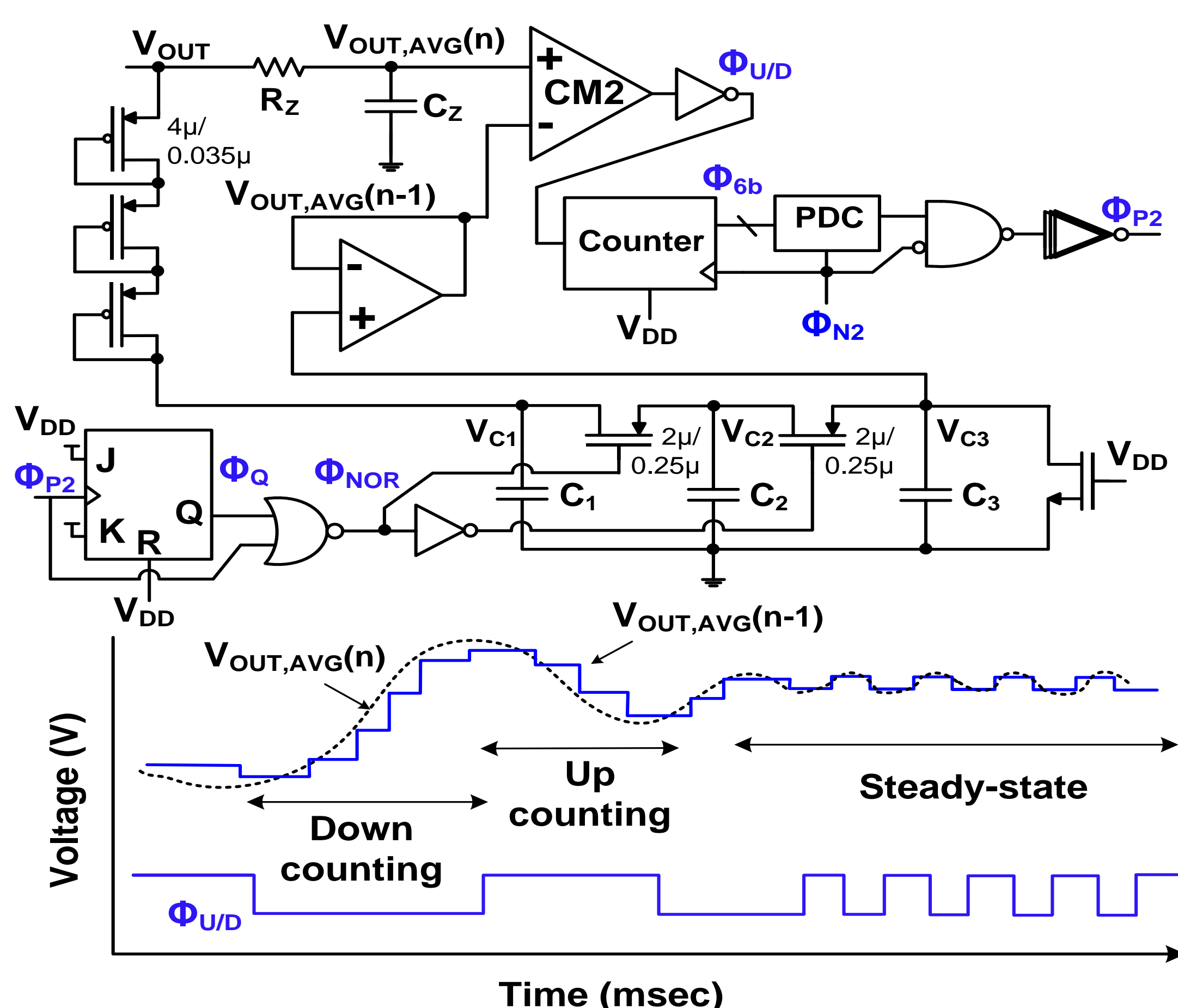


Fig. 4. Schematic diagram of the MOVT controller for I-ZCS.

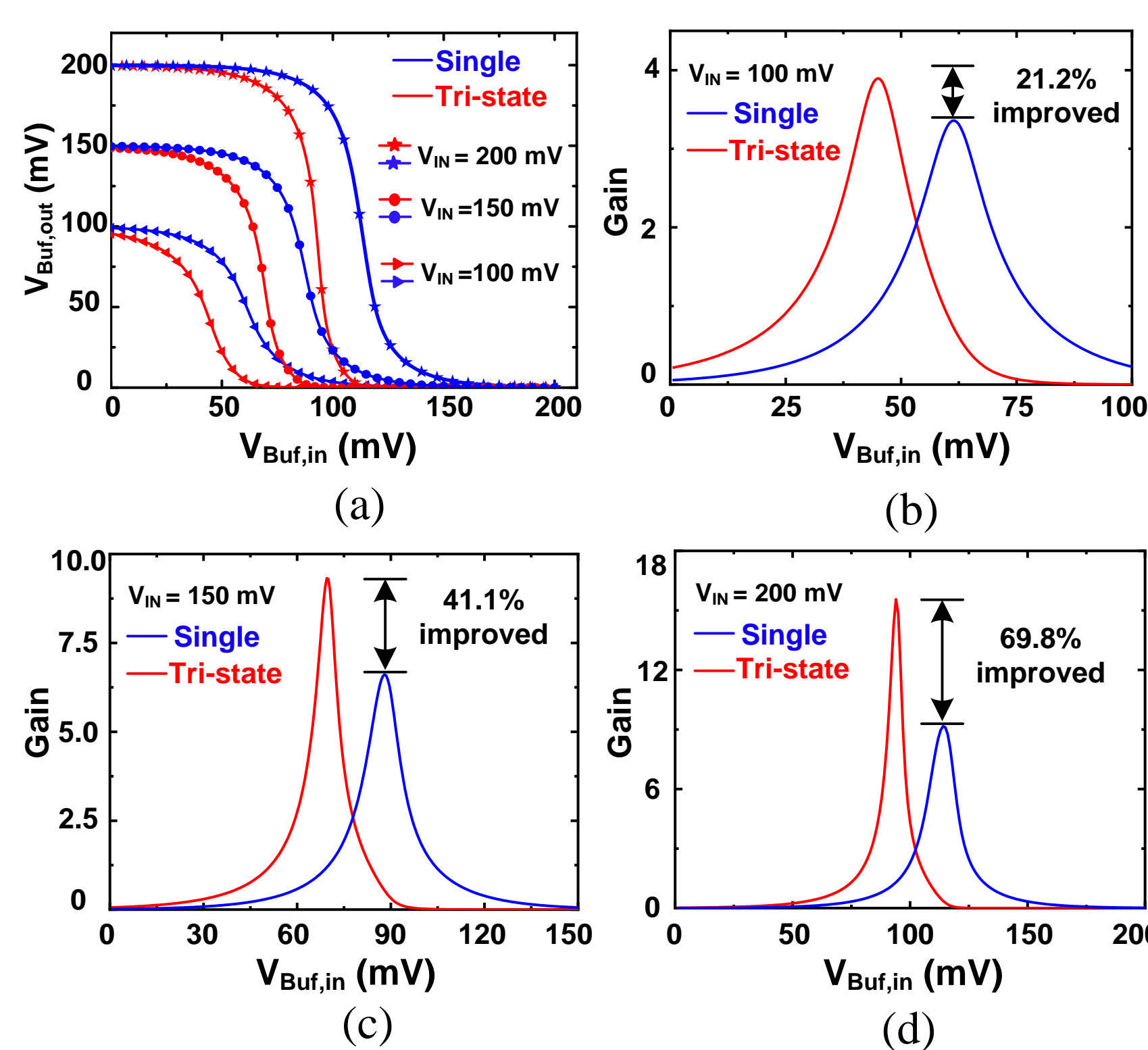


Fig. 3. (a) VTC comparison of the single and tri-state buffer, (b) DC gain comparison of the proposed tri-state buffer at $V_{IN} = 100$ mV, (c) at $V_{IN} = 150$ mV, (d) at $V_{IN} = 200$ mV.

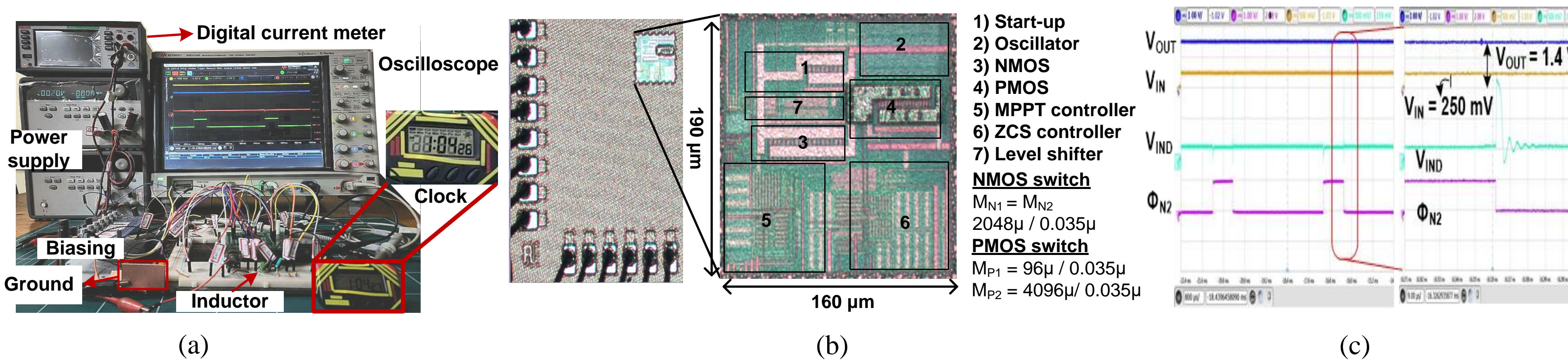


Fig. 5. (a) Measurement setup for powering the clock, (b) Die photograph of the fabricated converter, and (c) Measurement results.

Fig. 5(a) shows the measurement setup while powering the clock using the power supply voltage of 250 mV. Fig. 5(b) shows the micrograph of the boost converter consuming an active area of 0.3 mm^2 , and it is mounted on the test board using the chip-on-board (COB) technique. Fig. 5(c) shows the measurement of the boost converter operation. The experiment was performed using the supply source $V_{IN} = 250$ mV, $R_S = 20 \Omega$, and $C_{IN} = 0.47 \mu\text{F}$ and achieved the $V_{OUT} = 1.4$ V. The result shows the exact switching of M_{N2} to make sure the MPPT operation. The I-ZCS controller operation ensures accurate switching of the M_{P2} , as V_{IND} does not cross zero.

Conclusion

Table. 1 can conclude the performance of this design. Our work has a relatively high tracking efficiency (η_{MPPT}) than the other works [2,3]. The proposed work achieves the conversion efficiency (η_{CONV}) of 85.6% at the output power P_{OUT} . Our proposed startup achieved the minimum startup voltage of 90 mV. We achieved the $V_{OUT} = 1.4$ V while the $V_{IN} = 250$ mV and powered the clock.

References

- [1] S. S. Amin, et al, "MISMO: A multi-input single-inductor multi-output energy harvesting platform in 28-nm FDSOI for powering net-zero-energy systems," *IEEE JSSC*, Dec. 2018.
- [2] J. Jeong, et al, "A high-efficiency charger with adaptive input ripple MPPT for low-power thermoelectric energy harvesting achieving 21% efficiency improvement," *IEEE JSSC*, Jan. 2020.
- [3] S. C. Chandrarthna, et al, "A self-resonant boost converter for photovoltaic energy harvesting with a tracking efficiency > 90 % over an ultra-wide source range," *IEEE JSSC*, Jun. 2022.

Acknowledgement

The chip fabrication and CAD tools were supported by the IDECC (IC Design Education Center).

Fig. 1 shows the simplified schematic of the proposed system architecture, which consists of a startup circuit and boost converter with a shared inductor. The controller part of the boost converter consists of the maximum power point tracking (MPPT) controller and the I_ZCS controller, which controls the converter switches (M_{N2} and M_{P2}) respectively.

Fig. 2 shows the schematic of the proposed cold-startup circuit. The ring oscillator uses a tri-state buffer instead of a single buffer to achieve linear VTC and high gain for low voltage. The dc gain of the tri-state buffer is

$$A_{-}V_2 = \frac{g_{m,eff}}{g_{ds,P2} + g_{ds,N2}} \quad (1)$$

$$g_{m,eff} = (1 + A_{-}V_1)g_{m,P2} + g_{m,N2} \quad (2)$$

Fig. 3(a) shows the VTC comparison of the single and tri-state buffer at different V_{DD} levels, results show that the high gain has linear VTC. Fig. 3(b) shows the gain characteristics of a single and tri-state buffer at $V_{IN} = 100$ mV the improvement in dc gain is 21.2%. Fig. 3(c) shows the 41% improvement in the dc gain when $V_{IN} = 150$ mV. Fig. 3(d) shows that the tri-state buffer has a 69.8% dc gain improvement over a single buffer at $V_{IN} = 200$ mV.

Fig. 4 shows the schematic of the MOVT controller for the I-ZCS. It consists of a comparator that compares the current state of the average output voltage ($V_{OUT,AVG(n)}$) after the low pass filter with the previous state of the output voltage ($V_{OUT,AVG(n-1)}$). The time period t_p for the switch M_{P2} is

$$\Delta t_p = \frac{1}{t_N} \times \left[\frac{-\Delta V_{OUT} \times L}{V_{OUT} \times f_S \times R_{OUT}} \right] \quad (3)$$

Table 1. Performance comparison

	[2]	[3]	This work
Process	180 nm	180 nm	28 nm
Energy source	TEG	PV	TEG
Type	Boost	Boost	Boost
Startup technique	CP	CP	Ring OSC
Minimum startup voltage	500 mV	80 mV	90 mV
MPPT technique	[†] AIR	^{**} SRFG	FOCV
η_{MPPT}	98% @ $P_{IN} = 470 \mu\text{W}$	97% @ $P_{IN} = 1.125 \text{ mW}$	95.2% @ $P_{IN} = 615 \mu\text{W}$
η_{CONV}	82% @ $P_{OUT} = 394 \mu\text{W}$	89% @ $P_{OUT} = 0.12 \text{ mW}$	85.6% @ $P_{OUT} = 1.07 \text{ mW}$
V_{OUT}	1 - 1.2 V	1.2 V	1.4 V
Area (mm^2)	1.1	1.5	0.3

[†]Adaptive input ripple ^{**}Self-controlled resonant frequency generator